

# Hot Jupiters and Central Cavities of Protoplanetary Discs

Szymon Starczewski<sup>1</sup>, Artur J. Gawryszczak<sup>1</sup>,  
Richard Wünsch<sup>1,2</sup> & Michał Różyczka<sup>1</sup>

<sup>1</sup>N. Copernicus Astronomical Center, Warsaw, Poland

<sup>2</sup>Astronomical Institute, Academy of Sciences of the Czech Republic,  
Praha, Czech Republic

e-mail: (star, gawrysz, mnr)@camk.edu.pl  
richard.wunsch@matfyz.cz

## Abstract

We investigate numerically the orbital evolution of massive extrasolar planets within central cavities of their parent protoplanetary discs. Assuming that they arrive at the inner edge of the disc due to type II migration, we show that they spiral further in. We find that in magnetospheric cavities more massive planets stop migrating at a larger distance from the edge of the disc. This effect may qualitatively explain the correlation between masses and orbital periods found for massive planets with  $P$  shorter than 5 days.

**key words:** extrasolar planets, planet formation, protoplanetary discs

## 1 Introduction

The standard model of giant planet formation through core-accretion and envelope capture assumes that a solid core is formed first by accretion of planetesimals, and when it becomes massive enough it begins to accrete gas from the surrounding nebula. It is generally believed that gas giants form exterior to the snow line, i.e. where the disc is cold enough for water to condense, thus increasing the amount of solids available for core buildup (in very massive discs the cores can reach the critical mass also interior to the snowline). Once a sufficiently massive planet is formed, it opens a gap in the disc and undergoes migration of type II; see e.g. Ida & Lin (2004) and references therein. Less massive planets, unable to open a gap,

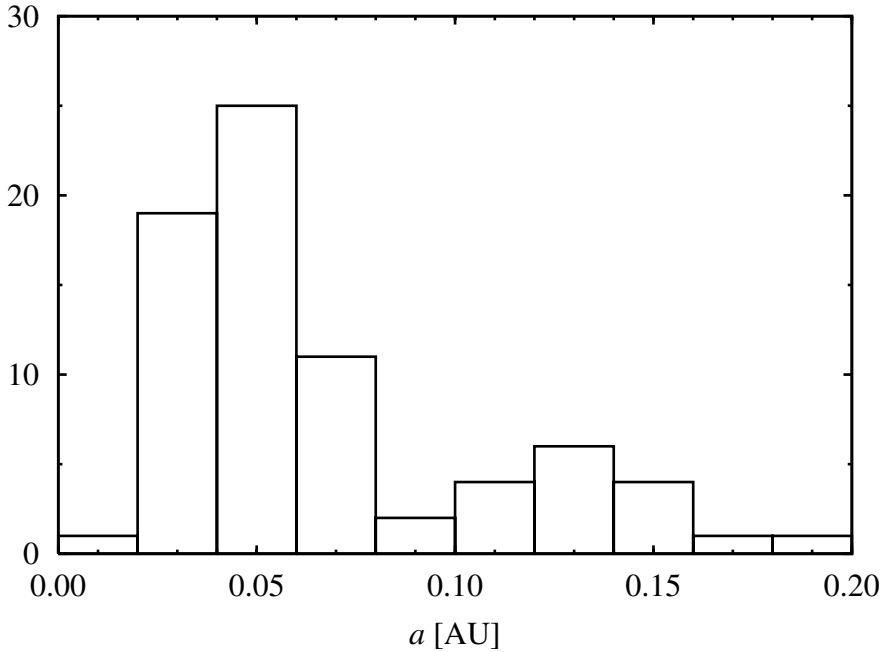


Figure 1: The histogram of semimajor axes of Hot Jupiters. Based on data from Schneider (2007).

are likely to undergo migration of type I; see e.g. Ward (1997). In either case, the final orbit of the planet is expected to be much tighter than the original one.

The prime candidates for planets that have undergone extensive migration are objects on the tightest orbits, whose orbital radii are clustered between  $a \approx 0.03$  a.u. and  $a \approx 0.06$  a.u. (Fig. 1). A major fraction of these objects are the so-called Hot Jupiters (hereafter HJ), i.e. giant gaseous planets of Jupiter or Saturn type. Several ideas have been proposed how to stop the migration at small orbital radii, including presence of a central cavity in the disc, tidal interactions with the star, and mass loss from the planet due to the Roche lobe overflow (Trilling et al. 1998). The cavity may originate due to the truncation the disc by the magnetosphere of the star (Lin, Bodenheimer & Richardson 1996; hereafter LBR) or the magnetorotational instability, which accelerates the accretion flow, leading to a strong drop in surface density up to the radius where the temperature falls below 1500 K (Kuchner and Lecar 2002).

The magnetospheric truncation hypothesis is strongly supported by the fact that T Tau stars have magnetic fields with intensities up to  $\sim 4.5 \times 10^3$  G (Symington et al. 2005). For typical accretion rates inferred for these objects ( $10^{-9}$  to  $10^{-7} M_{\odot} \text{ yr}^{-1}$ ) the disc should be truncated at a distance of a few  $R_{\star}$  (stellar radii) from the star. This prediction finds some observational support, as circumstellar

cavities of a few  $R_*$  are required to explain the widths of CO lines most likely originating in a gas on Keplerian orbits around T Tau stars (Bouvier et al. 2006 and references therein). An obvious conclusion is that many (perhaps most) HJs with semimajor axes smaller than  $\sim 0.06$  AU must have spent some time *within an active magnetosphere*, i.e. within the central cavity of their parent protoplanetary disc.

The orbital evolution of a planet within the magnetospheric cavity was considered by LBR. In their scenario, the disc is truncated at the magnetospheric radius  $r_m \approx 0.08$  AU. The star corotates with the inner edge of the disc, to which it is magnetically locked. A planet that has migrated into the cavity experiences negative torques from both the disc and the star. However, once it has spiralled past the 2:1 resonance at the orbital radius  $a_{2:1} = 0.63r_m$ , the torque from the disc becomes drastically weaker. The stellar torque also weakens in time due to the contraction of the star on its way to the main sequence (in fact, it may even reverse the sign if the angular momentum of the star is conserved). As a result, LBR expect the migration to effectively stop at  $\sim 0.05$  AU. The same basic scenario is repeated in many later papers, e.g. Lin et al. (2000), Kuchner & Lecar (2002), Eisner et al. (2005), Santos et al. (2005) or Romanova & Lovelace (2006). However, despite of its popularity, it has never been verified by numerical simulations.

LBR and their followers implicitly assume that i) the magnetosphere simply truncates the disc at  $r_m$ , leaving it undisturbed for  $r > r_m$ , and ii) the gravity of the matter accreting onto the star along the field lines and/or blown away from the star as a magnetized wind can be neglected. At a first glance, neither of these assumptions looks plausible; however they are quite strongly supported by several arguments. First, Romanova & Lovelace (2006) demonstrate that in many cases the magnetospheric cavity is indeed almost empty. Second, the simulations of Long, Romanova & Lovelace (2005; hereafter LRL) show that in many cases the gravity of the wind is indeed negligible (typical of their type II models is an outflowing corona with a density  $\sim 10^3$  times lower than the midplane density of the disc). Third, in some LRL models the accreting matter forms a nearly spherical thin shell with narrow polar funnels. If the shell is nearly uniform, then the gravitational potential it generates within the magnetosphere is nearly constant, and the gravitational effect of the accretion flow on the planet residing in the magnetosphere may be rather weak. Of course, because of numerous plasma instabilities, a smooth magnetospheric shell is an oversimplification. However, it is quite feasible that the time-averaged contribution to the torque on the planet from the fluctuating part of the density field is insignificant.

Based on these arguments, the magnetospheric migration can be followed by simplified simulations in which i) the accretion disc has a sharp inner edge at the magnetospheric radius  $r_m$ , ii) the matter that arrives at  $r_m$  does not enter the magnetosphere but is lifted off the disc, and iii) at  $r < r_m$  the net gravitational

effect of the magnetospheric flow is neglected. Following the implicit assumption made by LBR, we also assume that beyond  $r_m$  the disc is practically undisturbed by magnetic fields, i.e. that non-Keplerian effects in its dynamics are dominated by the gravity of the planet rather than Lorentz force. The latter assumption, whose validity we check *a posteriori* in Sect. 2.2, allows us to calculate the torque from the disc on the planet with the help of standard two-dimensional simulations.

The simulations are presented in Sect. 2. In Sect. 3 we discuss their results, and speculate about the origin of the semimajor axes distribution shown in Fig. 1. The paper is supplemented by an appendix containing a report on the code calibration test.

## 2 Numerical simulations

We employ the FLASH code, which operates on a *block-structured* grid (Fryxell et al. 2000). Within each block the equations of hydrodynamics are solved using a conservative third-order Eulerian scheme (Colella & Woodward 1984). FLASH can build a hierarchy of progressively finer grids by "halving" the blocks in each coordinate whenever refinement is required. For the present simulations, however, a uniform (nonrefined) grid proved to be sufficient.

### 2.1 Problem setup

We consider a system composed of a central star with mass  $M_*$  (in the simulations  $M_* = 1M_\odot$ ), a planet with mass  $M_p$ , and a thin non-selfgravitating disc truncated at a distance  $r_m$  from the star. The disc is locally isothermal, and the vertically integrated pressure  $p$  is related to the surface density  $\Sigma$  through

$$p = \Sigma c_s^2, \quad (1)$$

with the local sound speed given by

$$c_s = H\Omega_K, \quad (2)$$

where  $\Omega_K = \sqrt{GM/r^3}$  is the Keplerian angular velocity, and  $H$  is the half-thickness of the disc. The aspect ratio  $h \equiv H/r$  is assumed constant over  $r$  and equal to 0.05.

We do not introduce any explicit magnetic field. Following the arguments presented in Sect. 1, we simply assume that for  $r < r_m$  the accretion flow does not influence the planet in any way. With such an assumption, in a coordinate system centered on the star the orbital evolution of the planet is described by the standard equation

$$\frac{d^2 \mathbf{a}}{dt^2} = -\frac{G(M_* + M_p)}{a^3} \mathbf{a} - \nabla \Phi_d, \quad (3)$$

where  $\mathbf{a}$  is the position vector of the planet, and  $\Phi_d$  is the gravitational potential of the disc. The formula for the potential,

$$\Phi_d = -G \int_S \frac{\Sigma(\mathbf{r})}{|\mathbf{r} - \mathbf{a}|} d\mathbf{r} + G \int_S \frac{\Sigma(\mathbf{r})}{r^3} \mathbf{a} \cdot \mathbf{r} d\mathbf{r}, \quad (4)$$

contains the indirect term accounting for the non-inertiality of the coordinate system, and the integration in (4) is performed over the surface of the disc.

The magnetospheric radius is given by the standard formula

$$r_m = \eta \left( \frac{B_\star^4 R_\star^{12}}{G M_\star \dot{M}^2} \right)^{1/7}, \quad (5)$$

where  $B_\star$ ,  $R_\star$ ,  $M_\star$ ,  $\dot{M}$  and  $\eta$  are, respectively, field strength at the surface of the star, stellar radius, stellar mass, accretion rate, and a dimensionless factor of order unity. For a star with an aligned dipole field  $0.5 \leq \eta \leq 1.0$ ; see e.g. Lai (1999) and references therein. Normalized to the standard parameters of T Tau stars, equation (5) reads

$$\frac{r_m}{R_\odot} = 4.29\eta \left[ \frac{\left( \frac{B_\star}{1000 \text{ Gs}} \right)^4 \left( \frac{R_\star}{R_\odot} \right)^{12}}{\frac{M_\star}{M_\odot} \left( \frac{\dot{M}}{10^{-8} M_\odot/\text{yr}} \right)^2} \right]^{1/7}, \quad (6)$$

We take  $r_m = 12R_\odot = 0.056 \text{ AU}$ , which agrees with the distance range suggested by the distribution shown in Fig. 1 (note also that for the standard values of  $B_\star$ ,  $M_\star$  and  $\dot{M}$  the adopted value of  $r_m$  corresponds to an entirely reasonable range of stellar radii  $2R_\odot \leq R_\star \leq 3R_\odot$ ).

## 2.2 Results

The simulations were performed on a polar grid of  $n_r = 512$  and  $n_\phi = 128$  points, extending from  $r_{\text{in}} = r_m$  to  $r_{\text{out}} = 0.356 \text{ AU}$ . We checked that doubling  $n_r$  and  $n_\phi$  changes the value of the disc torque on the planet by less than 2%, which proved that our basic resolution was sufficient for the present problem. At  $r_{\text{in}}$  a free outflow boundary condition was applied, while at the outer edge of the disc we implemented the prescription proposed by de Val-Borro et al. (2006) to damp reflections from the boundary of the grid. Specifically, after each time-step the equation

$$\frac{dX}{dt} = -\frac{X - X_0}{P} R(r) \quad (7)$$

was solved, where  $X$  stands for  $\Sigma$  or velocity component,  $X_0$  is the initial profile of a particular variable, and  $R(r)$  is a parabolic ramp function which decreases

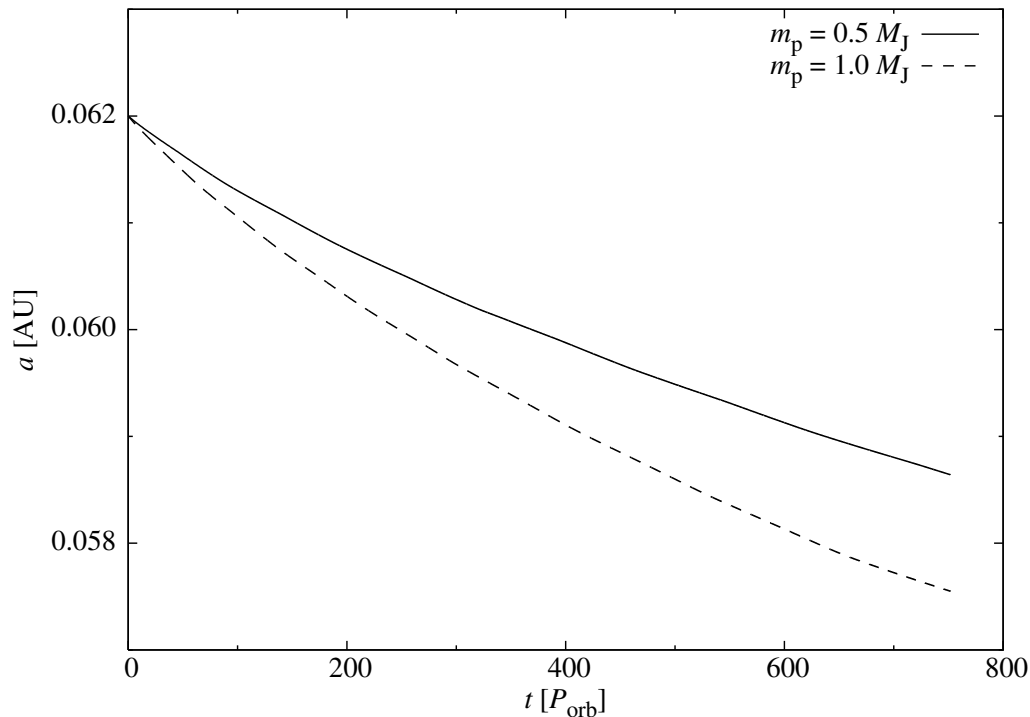


Figure 2: The migration of planets in a disc with  $M_d = 10M_J$ . Solid:  $M_p = 0.5M_J$ . Dashed:  $M_p = 1M_J$ .

smoothly from 1 at  $r = r_{\text{out}}$  to 0 at  $r = 0.84r_{\text{out}}$ . The default FLASH artificial viscosity with  $c_{\text{visc}} = 0.1$  was used to stabilize the solution.

Initially the disc is uniform, and  $a = 0.062$  AU. To relax the model, we keep the planet on the initial orbit until it carves a quasistationary gap in the disc, exterior to which a spiral density pattern emerges. When the relaxation procedure is completed (usually after  $\sim 100$  orbital periods of the planet), the time-counter is reset to 0, and the planet begins to evolve according to equation (3) which we integrate with a fourth-order Runge-Kutta scheme. We performed simulations for two values of the mass of the planet ( $M_p = 0.5M_J$  and  $M_p = 1M_J$ , where  $M_J$  is the mass of Jupiter), and two values of the mass of the disc contained in the grid ( $M_d = 10M_J$  and  $M_d = 100M_J$ ). The latter were chosen unrealistically large in order to speed the evolution up, so that noticeable effects could be produced in a reasonable CPU time. Within the adopted scenario the gravitational torque  $T$  from the disc on the planet should scale linearly with  $M_d$ , and this is what we observe in our simulations. Thus, the fact that our discs are far too massive does not influence the conclusions of the paper.

As soon as the planet has been released from its initial orbit, it begins to migrate into the magnetosphere. The migration process is illustrated in Figs. 2 and 3

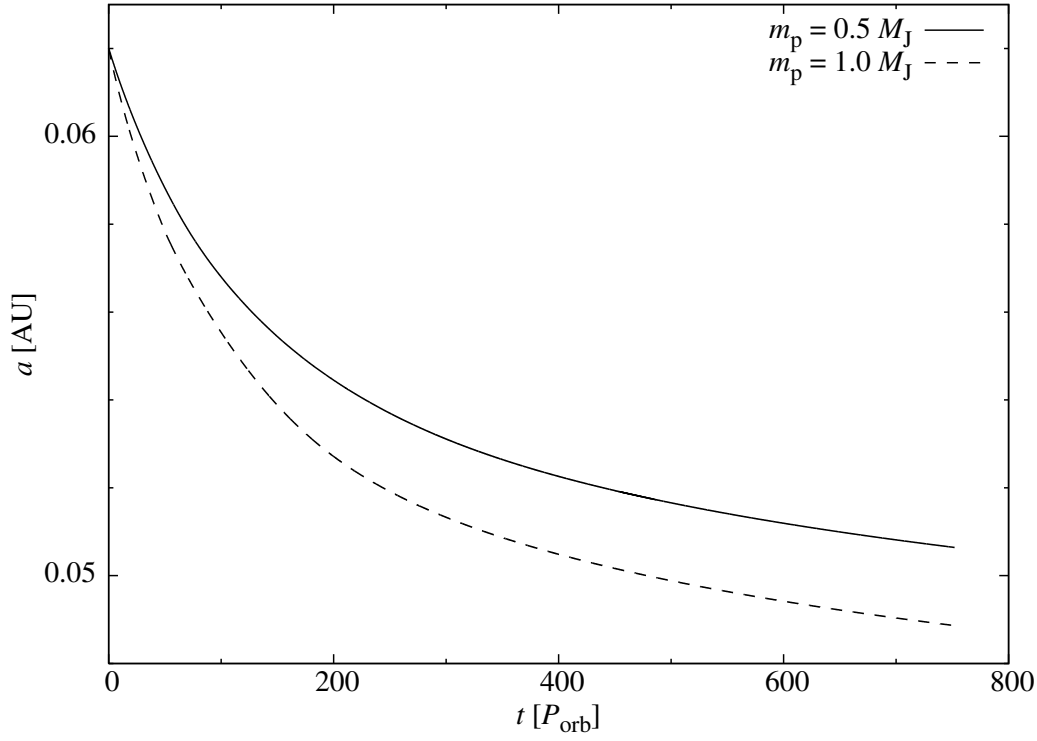


Figure 3: As in Fig. 2, but in a disc with  $M_d = 100M_J$

for discs with  $M_d = 10M_J$  and  $M_d = 100M_J$ , respectively. As expected, a planet with given  $M_p$  migrates faster in more massive discs. Figs. 2 and 3 also demonstrate that in a disc with given  $M_d$  the migration rate is faster for more massive planets.

Finally, in Fig. 4 we plot  $|T|$  as a function of  $r$  for both values of  $M_p$  (note that after an initial adjustment the torque scales with  $M_p^2$ ). In the following we argue that for realistic values of  $M_{d,p}$  the gravitational torque is comparable to or weaker than the magnetic torque  $T_m$  on the disc from the star. In the following,  $T$  and  $T_m$  will stand for absolute values of gravitational and magnetic torque, respectively.

The centrally peaked minimum mass solar nebula (MMSN) with the surface density profile

$$\Sigma_1 = 10^3 \text{ g cm}^{-2} \left( \frac{r}{\text{AU}} \right)^{-3/2} \quad (8)$$

(Ruden 1999), and the more gently peaking disc simulated by Nelson et al. (2000), with the profile

$$\Sigma_2 = 10^3 \text{ g cm}^{-2} \left( \frac{r}{\text{AU}} \right)^{-1/2} \quad (9)$$

yield, correspondingly,  $M_d \approx 1.5M_J$  and  $M_d \approx 0.03M_J$ . For further estimates we take the geometrical mean of these two values, i.e.  $M_d = 0.2M_J$ . The standard

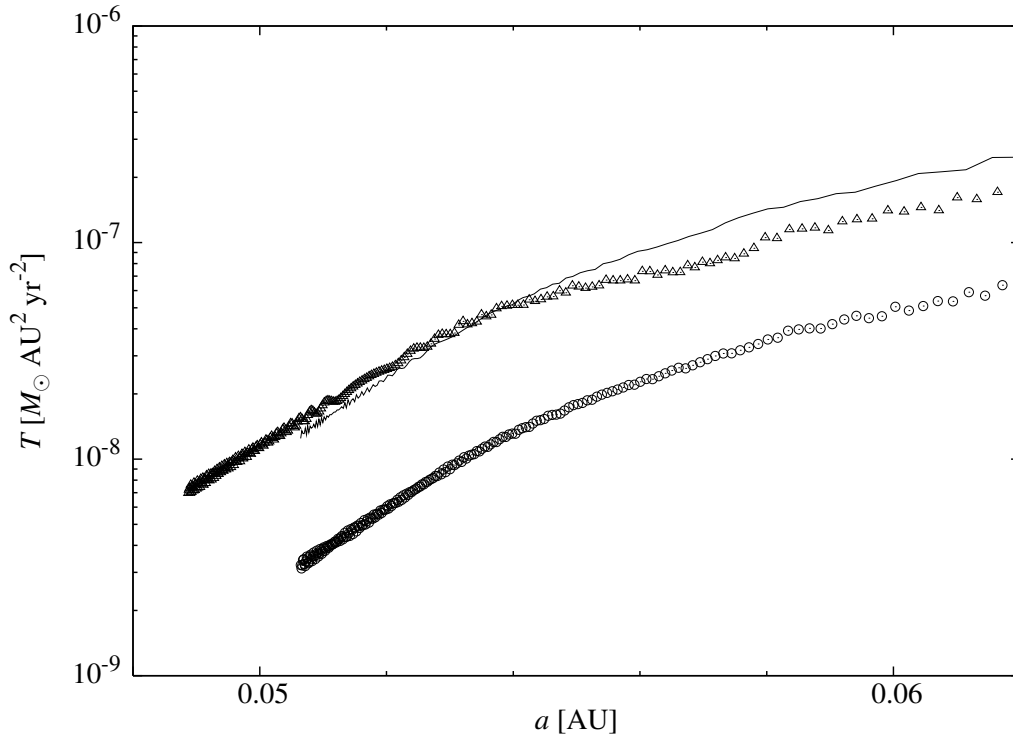


Figure 4: The absolute value of the disc torque on the planet as a function of the distance from the central star. Triangles:  $M_p = 1 M_J$ . Circles:  $M_p = 0.5 M_J$ . Thin line: torques for  $M_p = 0.5 M_J$  multiplied by 4. Vertical axis: values obtained from the simulation with  $M_d = 100 M_J$ , scaled to  $M_d = 0.2 M_J$ .

formula for  $T_m$

$$T_m = \frac{B_\star^2 R_\star^6}{r_m^3} \quad (10)$$

(Lai 1999) contains weakly constrained parameters  $B_\star$  and  $R_\star$ . However, using (5) with  $\eta = 1$  we see that the characteristic time scale

$$\tau_m \equiv \frac{J_p(r_m)}{T_m} = \frac{M_p \sqrt{GM_\star r_m} r_m^3}{B_\star^2 R_\star^6} = \frac{M_p}{\dot{M}} \quad (11)$$

(where  $J_p(r_m)$  is the orbital angular momentum of the planet at the edge of the magnetosphere), does not depend on  $B_\star$  or  $R_\star$ . For  $M_p = 1 M_J$  and  $\dot{M} = 10^{-8} M_\odot \text{ yr}^{-1}$  equation (11) yields  $\tau_m = 10^5 \text{ yr}$ . This is the time scale on which a planet placed at  $r_m$  would migrate if the torque from the disc was equal to  $T_m$ . We shall compare it with the timescale of migration due to the gravitational torque,  $\tau_g \equiv J_p(r_m)/T$ .

The orbital angular momentum of a  $1 M_J$  planet placed at  $r_m = 0.056 \text{ AU}$  is equal to  $1.5 \times 10^{-3} M_\odot \text{ AU}^2 \text{ yr}^{-1}$ . From Fig. 4 we have  $T(r_m) = 7.5 \times 10^{-8} M_\odot \text{ AU}^2 \text{ yr}^{-2}$ ,



yielding  $\tau_g = 2 \times 10^4$  yr. Thus,  $T = 5T_m$ , and the assumptions of Sect. 1 are satisfied. However, already when the planet has migrated to  $a = 0.9r_m = 0.05$  AU,  $T$  drops to  $10^{-8} M_\odot \text{AU}^2 \text{yr}^{-2}$ , and  $\tau_g$  increases to  $1.5 \times 10^5$  yr. This means that  $T_m$  is now larger than  $T$ , i.e. the inner edge of the disc is more strongly influenced by MHD effects rather than gravity. For the  $0.5M_J$  planet the situation is even worse, since  $T \approx T_m$  already at  $r_m$ . As the disc dominated by chaotic MHD effects cannot exert a consistent negative torque on the planet, we conclude that planets with  $M_p \leq 0.5M_J$  are unable to spiral into the magnetosphere, whereas Jupiter-size planets stop spiralling at a distance  $\sim 0.006$  AU from the inner edge of the disc.

### 3 Discussion

Based on the data from the beginning of September 2004, Mazeh, Zucker and Pont (2005); hereafter MZP, and Gaudi et al. (2005) found that among 6 then-known transiting HJs more massive planets tended to have shorter periods. The same effect was visible in the whole population of 17 then-known planets with orbital periods shorter than 5 days (hereafter: SPP), albeit with large scatter. Presently (end of May 2007) 46 SPP are known (47<sup>th</sup> object with  $P < 5^d$  is a brown dwarf HD41004 B b), 20 of which are transiting (Schneider 2007), and it is interesting to see whether the original correlation still persists.

Following MZP, we exclude planets in known binary systems ( $\tau$  Boo b and HD 188753A b) as well as "Hot Neptunes" (GJ 436 b, 55 Cnc e, Gliese 876 d, GJ 674 b and HD 219828 b), which, as MZP write, "probably are of a different nature and have a different formation and evolutionary history". We also exclude three transiting objects: SWEEPS-04, whose RV amplitude is insignificant, SWEEPS-11, which seems to be a brown dwarf rather than a planet (Sahu et al. 2006), and XO-3, whose mass is at the lower limit of the brown-dwarf range, and whose orbit is highly eccentric. Amazingly, the slope of the linear fit to the  $M_p(P)$  relation found for the 14 transiting planets with reliably determined masses is nearly the same as the one found by MZP (Fig.5). Moreover, the correlation is also visible for the whole sample of SPP, and the slope also nearly the same. MZP could not provide any explanation for the observed effect, and suggested that such an explanation should be worked out when the  $M_p - P$  correlation is better established. As the new data confirm their findings, the effect seems to be ripe for consideration.

Because masses of stars orbited by SPP are rather tightly clustered around  $1 M_\odot$ , whereas masses of SPP are at least several hundred times smaller, periods of SPP are primarily determined by their orbital radii. As a result, the  $M_p - P$  correlation implies a similar connection between masses and orbital radii, which is indeed observed (Fig. 6). We have shown that the "classical" scenario of the orbital evolution inside the magnetosphere, in which planets stop migrating at

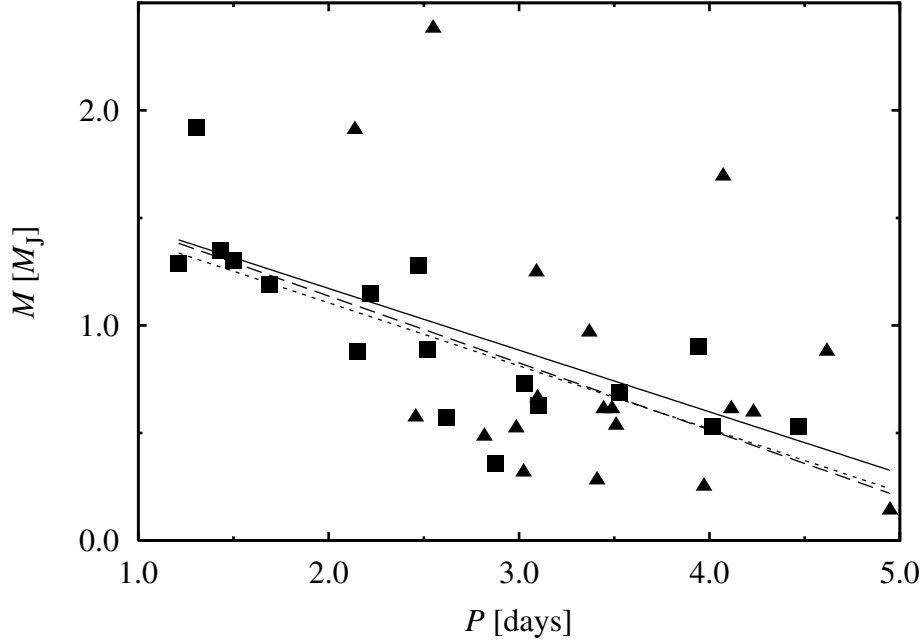


Figure 5: The mass-period relation for planets with periods shorter than 5 days. Based on data from Schneider (2007). Squares: transiting planets. Triangles: planets for which spectroscopic data are only available (as in MZP, their lower mass limits are divided by  $\pi/4$ , the expected value of  $\sin i$ ). Dotted, dashed and solid line: fits to, correspondingly, 6 transiting planets of MZP, 17 transiting planets with reliably determined masses known in January 2007, and all SPP known at the end of May 2007.

$\sim 0.63r_m$ , is not true. Moreover, even if it were correct, it would not be able to account for the observed effects. To see it, imagine an evolving population of planets represented by points scattered on the  $(a, M_p)$  plane. Initially, every planet resides at its  $r_m$ . We do not know the distribution of  $r_m$ , but it seems reasonable to assume that it is flat between some  $r_{m,\min} < 0.056$  AU and  $r_{m,\max} \approx 0.056$  AU. If this is so, then 1) at  $t = 0$  there's no correlation between  $M_p$  and  $a$ , and 2) such correlation cannot emerge for any  $t > 0$ , because every point is displaced horizontally by an amount which depends on  $r_m$ , but does not depend on  $M_p$ .

If the cavities are not of magnetospheric origin, but originate from increased viscosity and accelerated accretion flow (Kuchner and Lecar 2002), we encounter another problem. Although in this case the disc is not perturbed by the magnetic field of the star, its inner part may be strongly unstable, causing the edge of the cavity to irregularly or semi-regularly change its location (Wünsch et al. 2006). As a result, any correlation between  $M_p$  and  $a$  or  $P$  is highly unlikely.

The results of our simulations imply however that more massive planets tend to stop deeper in the magnetosphere, and in the following we argue that this effect can at least qualitatively account for the observed correlations. If the disc conforms to the simple  $\alpha$ -model, then the velocity of the accretion flow is given by

$$v_r = \alpha h^2 r \Omega_K, \quad (12)$$

and, provided that  $\alpha$  and  $h$  do not change, the accretion rate

$$\dot{M} = 2\pi\alpha h^2 r^2 \Omega_K \Sigma \quad (13)$$

scales proportionally to  $\Sigma$ . This means that by varying  $\dot{M}$  at a constant  $r_m$  we do not change the timescale ratio  $\tau_g/\tau_m$ , i.e. the conclusions of Sect. 2 remain valid when the surface density is decreased or increased at the inner edge of the disc.

As the planet recedes from the inner edge of the disc, its tidal effect on the disc approaches the linear regime in which the density perturbation  $\Delta\Sigma$  is small compared to the unperturbed density  $\Sigma_0$ . Eventually,  $T$  should converge to the linear torque which scales proportionally to  $aM_p^2$  (Ward 1997), and Fig. 4 shows that it is indeed the case. Based on a particle approximation, the same scaling was found by Lin and Papaloizou (1978) for the case of a small-mass component of a binary with an external (i.e. circumbinary) disc. (Strictly speaking, the formula given by Ward concerns the *net torque* on the planet, but the torque components originating exterior and interior to the orbit scale in the same way). After some algebra we see that timescale ratios of planets with masses  $M_{p1}$  and  $M_p$  which begin to spiral into cavities whose edges are located, correspondingly, at  $r_{m1}$  and  $r_m$ , are related by the formula

$$\frac{\tau_{g1}}{\tau_{m1}} = \left( \frac{M_p}{M_{p1}} \right)^2 \sqrt{\frac{r_m}{r_{m1}}} \frac{\tau_g}{\tau_m}. \quad (14)$$

Since we have found that  $\sim 0.5M_J$ -planets are hardly able to detach from the edge of the cavity, we may assume based on Fig. 6 that the radii of the smallest cavities were not much different from  $\sim 0.036$  AU. Let us consider two identical planets, the first one spiralling into our "standard" magnetosphere with  $r_m = 0.056$  AU, and the second one into the "compact" magnetosphere with  $r_{m1} = 0.036$  AU. According to equation (14), for the second planet the ratio  $\tau_g/\tau_m$  is just by  $\sim 25\%$  larger than for the first one. As a result, both planets reach a similar stopping distance  $d_s$  from the edge of the disc, and to a first approximation we may assume that the function  $d_s(M_p, r_m)$  does not depend on  $r_m$ .

According to Marcy et al. (2005), the distribution of planetary masses is affected very little by the unknown inclination of orbits, and based on available data, one may adopt

$$dN(M_p) \sim M_p^{-1} dM_p. \quad (15)$$

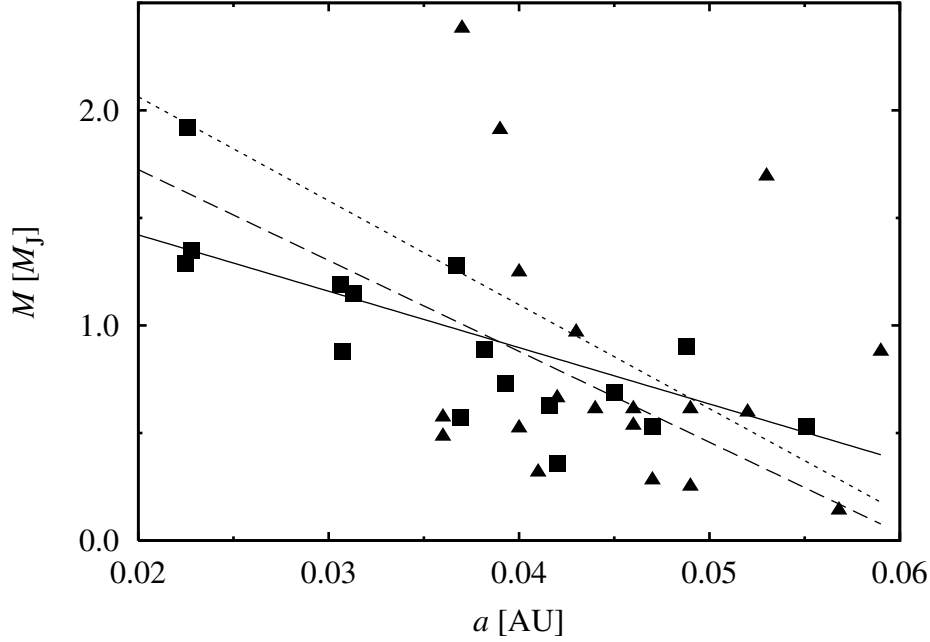


Figure 6: The mass - semimajor axis relation for the same planets as in Fig. 5. Solid, dotted, and dashed line: fits to, correspondingly, all SPP known at the end of May 2007, final  $(a, M_p)$  distribution for  $dN(M_p) \sim M_p^{-1} dM_p$ , final  $(a, M_p)$  distribution for  $dN(M_p) \sim M_p^{-2} dM_p$ .

As we have mentioned before, the distribution of magnetospheric radii is unknown, but since there is no obvious reason to favour any value of  $r_m$  we may assume that all values between  $r_{m1}$  and  $r_m$  are equally probable. With these assumptions, the joint distribution of  $M_p$  and  $r_m$  is given by

$$F(M_p, r_m) = \mathcal{N} M_p^{-1} \chi_1(M_p) \chi_2(r_m), \quad (16)$$

where  $\chi_1(x) = 1$  for  $0.5 \leq x \leq 2.5$  and 0 otherwise ( $2.5 M_J$  is the estimated mass of the most massive SPP in Fig. 6),  $\chi_2(x) = 1$  for  $0.036 \leq x \leq 0.056$  and 0 otherwise, whereas

$$\mathcal{N} = \left( \int_0^\infty \int_0^\infty m^{-1} \chi_1(m) \chi_2(x) dx dm \right)^{-1}. \quad (17)$$

The ratio  $\tau_g/\tau_m$  decreases rather sharply with the increasing mass of the planet, but in order to remain on the conservative side we may adopt that the stopping distance scales linearly with  $M_p$ , according to the formula

$$\frac{d_s}{\text{AU}} = 0.012 \frac{M_p}{M_J} - 0.006, \quad (18)$$

which in agreement with our results yields  $d_s = 0$  AU for  $M_p = 0.5M_J$  and  $d_s = 0.006$  AU for  $M_p = 1M_J$ .

Let us again imagine an evolving population of planets represented by points scattered on the  $(a, M_p)$  plane. Every planet begins to spiral down from its  $r_m$ , and stops at  $a_s = r_m - d_s$ , with  $d_s$  depending primarily on the planet's mass. Thus, the final distribution of points is skewed toward smaller  $a$ , i.e. a correlation between  $M_p$  and  $a$  is generated. The least-square linear fit to the final distribution

$$M_p = \alpha * a + \beta \quad (19)$$

is given by the standard formulae

$$\begin{aligned} \alpha &= \frac{\int_0^\infty \int_0^\infty (m - \bar{M}_p) * [(x - d_s(m)) - (\bar{r}_m - \bar{d}_s)] F(m, x) dx dm}{\int_0^\infty \int_0^\infty [(x - d_s(m)) - (\bar{r}_m - \bar{d}_s)]^2 F(m, x) dx dm} \\ \beta &= \bar{M}_p - \alpha * (\bar{r}_m - \bar{d}_s), \end{aligned} \quad (20)$$

and is shown in Fig. 6. For comparison, analogous fit obtained for a steeper mass distribution  $dN(M_p) \sim M_p^{-2} dM_p$  is also plotted. Given the simplicity of our approach, the qualitative agreement of theoretical fits with the observational one looks quite encouraging.

So far we have neglected tidal interactions between the planet and the star. Following LBR and recent theoretical as well as observational evidence (Bouvier et al. 2006; Herbst & Mundt 2005, and references therein) we assume that T Tauri stars are rotationally locked to inner edges of their accretion discs. Since a locked star rotates at  $\Omega_\star \approx \Omega(r_m) < \Omega_p$ , the resulting stellar torque onto the planet is negative, causing orbital radius of the planet to evolve according to the formula

$$a(t)^{6.5} = a(0)^{6.5} - \frac{13}{2} \frac{3k_2^\star M_p}{Q_\star M_\star} R_\star^5 \sqrt{GM_\star} t; \quad (21)$$

see e.g. Pätzold et al. (2004). For  $M_\star = M_\odot$  we have

$$x(t)^{6.5} = x_0^{6.5} - 3.2 \times 10^{-6} \frac{M_p}{M_J} \left( \frac{R_\star}{R_\odot} \right)^5 t, \quad (22)$$

where  $x \equiv a/R_\odot$ ,  $t$  is expressed in years, and a value of  $1.2 \times 10^8$  was adopted for  $Q_\star/k_2$  (Pätzold et al. 2004). Under the influence of stellar tides alone a  $1 M_J$  planet departing from the edge of the magnetosphere at  $r_m = 0.056$  AU would spiral down to the surface of a  $3R_\odot$  star within  $\sim 1.3 \times 10^{10}$  yr, whereas for the same planet departing from  $r_{m1} = 0.036$  AU the spiralling would take  $\sim 7.5 \times 10^8$  yr. In fact, the spiralling time would be even longer because the star contracts, causing the stellar torque on the planet to decrease. According to Allain (1998),

within  $\sim 10^7$  yr  $R_\star$  can easily shrink by a factor of 5 if the star does not accrete, and when accretion is allowed for the contraction proceeds even more quickly (Siess et al. 1999). As a result, it is highly unlikely for stellar tides to significantly influence the orbital evolution of the planet within the disc lifetime.

On the other hand, equation (21) predicts a faster evolution for more massive planets, and assuming that  $\Omega_\star$  remains smaller than  $\Omega_p$  one might expect that Fig. 5 is just a snapshot of a distribution undergoing slow secular changes due to stellar tides. However, at the end of the pre–Main Sequence phase the radius of the star is equal to  $\sim R_\odot$ , and the stellar torque on the planet strongly decreases. As a result, the spiraling timescale of a  $1 M_J$  planet from  $r_{\text{m1}} = 0.036$  AU lengthens to well above  $10^{10}$  yr.

In the final note we would like to stress that we do not claim that the problem of correlation between SPP masses and periods has been solved. We merely report a mechanism which may qualitatively account for the observed trend. An alternative mechanism was discussed by Faber, Rasio & Willems (2005) and Rasio & Ford (2006), who argue that SPP are likely to have originated from the tidal capture of planets on originally highly eccentric orbits. It is also possible that both mechanisms have been at work; provided, of course, that the correlation is real and will be confirmed by future observations.

## Acknowledgments

This work was supported through grant 1P03D 02626 from the Polish Ministry of Science and by the European Research Training Network "The Origin of Planetary Systems" (contract number HPRN-CT-2002-00308). The software used in this work was in part developed by the DOE-supported ASC / Alliance Center for Astrophysical Thermonuclear Flashes at the University of Chicago. The simulations were partly performed at the Interdisciplinary Centre for Mathematical and Computational Modeling in Warsaw.

## References

- Allain, S. 1998, *Astron. & Astrophys.* 333, 629
- Bouvier, J., Alencar, S.H.P., Harries, T.J., Johns-Krull, C. M., Romanova, M.M. 2006, *Protostars and Planets V*, in press
- Colella, P., Woodward, P.R. 1984, *J. Comp. Phys.* 54, 174
- de val-Borro M., Edgar, R., Gawryszczak, A. et al. 2006, *MNRAS* 370, 529
- Eisner, J. A., Hillenbrand, L. A., White, R. J., Akeson, R. L., Sargent, A. I. 2005, *ApJ* 623, 952

- Faber, J. A., Rasio, F. A., Willems, B. 2005, *Icarus* 175, 248
- Ford, E. B., Rasio, F. A. 2006, *ApJ* 638, L45
- Fryxell, B., Olson, K., Ricker, P. et al. 2000, *ApJS* 131, 273
- Herbst, W., Mundt, R. 2005, *ApJ* 633, 967
- Ida, S., Lin, D.N.C. 2004, *ApJ* 604, 388
- Kuchner, M. J., Lecar, M. 2002, *ApJ* 547, L87
- Lai, D. 1999, *ApJ* 524, 1030
- Lin D. N. C., Bodenheimer P., Richardson D. C. 1996, *Nature* 380, 606
- Lin D. N. C., Papaloizou, J. 1978, *MNRAS* 186, 799
- Lin, D. N. C., Papaloizou, J. C. B., Terquem, C., Bryden, G., Ida, S. 2000, *Protostars and Planets IV* p. 1111, Arizona Univ. Press
- Long M., Romanova M.M., Lovelace R.V.E. 2005, *ApJ* 634, 1214
- Marcy G., Butler R. P., Fischer, D., Vogt, S., Wright J. T., Tinney C. G., Jones H. R. A. 2005, *Progr. Theor. Phys. Suppl.* 158, 24
- Mazeh T., Zucker S., Pont F. 2005, *MNRAS* 356, 955
- Nelson R. P., Papaloizou J. C. B., Masset F. Kley W. 2000, *MNRAS* 318, 18
- Romanova M. M., Lovelace R.V.E. 2006, *Protostars and Planets V*, in press
- Ruden, S.P. 1999, in "The Origins of Stars and Planetary Systems", eds. C.J. Lada and N.D. Kylafis, (Dordrecht: Kluwer), p. 64
- Sahu, K. C. et al. 2006, *Nature* 443, 534
- Santos, N. C., Benz, W., Mayor, M. 2005, *Science* 310, 251
- Schneider, J. 2007, *The Extrasolar Planets Encyclopaedia*, <http://exoplanet.eu/>
- Siess, L., Forestini, G., Bertout, C. 1999, *Astron. & Astrophys.* 342, 480
- Symington, N.H. Harries, T.J., Kurosawa, R., Naylor, T. 2005, *MNRAS* 358, 977
- Trilling, D.E., Benz, W., Guillot, T. et al. 1998, *ApJ* 500, 428
- Ward, W. R. 1997, *Icarus* 126, 261
- Wünsch, R., Gawryszczak, A. J., Klahr, H., Różyczka, M. 2006, *MNRAS* 367, 773

## Appendix: Code testing

Before the version of FLASH adapted to the problem of disc – planet interaction was used for the proper simulations, we had tested it for compatibility with analytical expressions for the disc torque on the planet obtained by Ward (1997).

Consider a thin disc with a surface density  $\sigma(r, \phi)$ , orbiting a central star of mass  $M_*$ . The mass of the disc is minute compared to  $M_*$ , and its self-gravity is negligible, causing orbital velocity and epicyclic frequency of the disc matter,  $\Omega$  and  $\kappa$ , to be nearly Keplerian. Assume that the temperature distribution in the disc does not depend on time, with the local sound speed  $c_s$  fixed according to (2). The disc is perturbed by a planet of mass  $M_p = \mu M_*$ , which moves around the star on

a circular orbit of radius  $a$ . As the perturbations are nonaxisymmetric, the planet is subject to a gravitational torque  $T$  from the disc. According to Ward (1997), the torque density  $dT/dr$  is given by

$$\frac{dT}{dr} = \epsilon \frac{2\mu^2(\sigma a^2)(a\Omega_p)^2 m_r^4 \psi^2}{r(1 + 4\xi^2)} \left( \frac{\Omega_p}{\kappa} \right)^2, \quad (23)$$

where  $\Omega_p$  is the angular orbital velocity of the planet,  $\xi = m_r c_s / r \kappa$ , and  $\epsilon$  is equal to  $+1$  ( $-1$ ) for torques originating in the disc interior (exterior) to the planet's orbit. The function  $m_r$  is given by the formula

$$m_r = \sqrt{\frac{\kappa^2}{(\Omega - \Omega_p)^2 - c_s^2/r^2}} = \left[ \left( 1 - \sqrt{\frac{r^3}{a^3}(1 + h^2)} \right)^2 - h^2 \right]^{-1/2}, \quad (24)$$

where  $\Omega^2 = \Omega_K^2 - c_s^2/r^2$  and (2) were used; whereas the function  $\psi$  – by the formula

$$\psi = \frac{\pi}{2} \left[ \frac{1}{m_r} \left| \frac{db_{1/2}^m(x)}{dx} \right| + 2\sqrt{1 + \xi^2} b_{1/2}^m(x) \right], \quad (25)$$

where  $b_{1/2}^m(x)$  is the Laplace coefficient with argument  $x = r/a$ .

To calculate the torque density from the numerical models, we integrate contributions from all grid cells forming a thin annulus at a distance  $r$  from the star :

$$\frac{dT}{dr} = G \int_0^{2\pi} \frac{M_p r \sin(\phi - \phi_p)}{d^2 + \varepsilon^2 r_R^2} \sigma(r, \phi) r d\phi, \quad (26)$$

where

$$d = \sqrt{a^2 + r^2 - r \cos(\phi - \phi_p)} \quad (27)$$

is the distance between the planet and the point  $(r, \phi)$  on the annulus;  $\phi_p$  stands for the positional angle of the planet,  $r_R$  is the Roche radius, and  $\varepsilon$  is a dimensionless softening parameter.

For the test runs we adopted  $M_p = 10 M_E$  (Earth mass) and  $a = r_m$ . The calculations were performed on a polar grid  $(r, \phi)$  extending radially from 0.03 to 0.18 AU. The disc had a constant surface density  $\sigma = 2.28 \times 10^5 \text{ g cm}^{-2}$ , so that the corresponding mass of the disc matter contained within the grid was equal to  $2.5 M_J$  (Jupiter mass). The softening parameter  $\varepsilon$  was set to 0.6. No explicit viscosity was used, and no special treatment was applied to the matter within the Roche lobe of the planet. The disc gas could flow freely through the radial boundaries of the grid.

We ran two test simulations with different resolutions. The results are shown in Fig. 7, from which it is evident that on the finer grid ( $512 \times 256$  points) the code



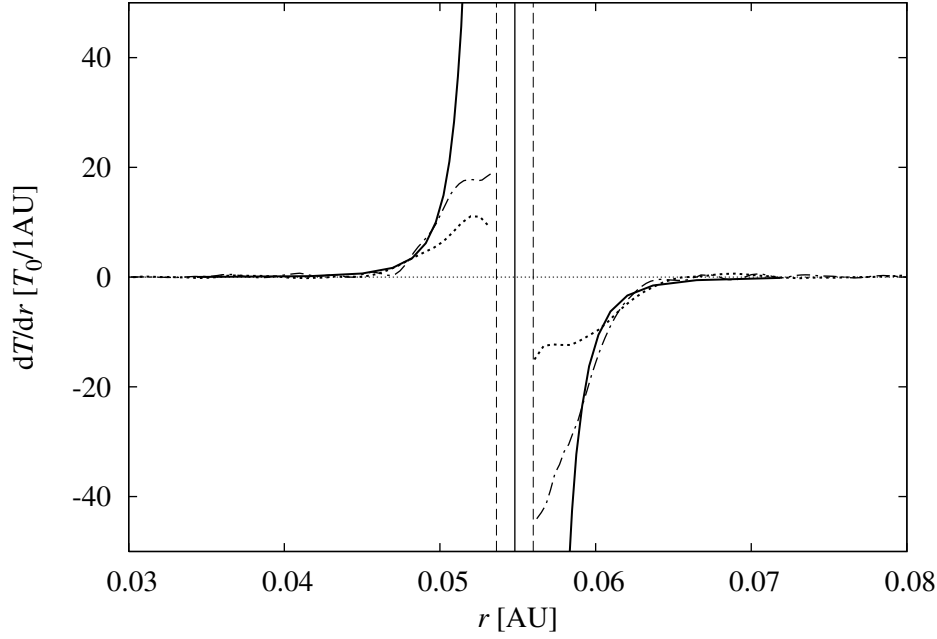


Figure 7: Torque densities obtained numerically for  $n_r \times n_\phi = 256 \times 128$  points (dotted) and  $512 \times 256$  points (dash-dotted), compared with the analytical solution (solid). Vertical lines: location of the planet (solid) and the torque cut-off limits at the Roche radius (dashed).  $T_0$  is the normalized torque defined as  $T_0 = \pi \mu^2 \sigma a^2 (a \Omega_p)^2 (a/h)^3$ . The plotted values are averages from 100 time steps (roughly one radian of the orbit).

is able to calculate reasonably accurate torques from the parts of the disc that are more distant than  $\sim 0.005$  AU or  $\sim 10$  grid cells from the planet. Since that area contributes less than 20% of the total torque from the disc, it may seem rather discouraging. The obvious conclusion is that if the planet is not able to open a gap, a really very high resolution is necessary to follow its migration through the disc. Obviously, for gap-opening planets the resolution requirements are much less stringent.